Electrical Capacitance Tomography for Level Measurements of Separated Liquid Stacks

M. Neumayer and H. Zangl
Institute of Electrical Measurement and Measurement Signal Processing
Graz University of Technology, Kopernikusgasse 24/IV, 8010 Graz, Austria
Email: neumayer@tugraz.at

I. Introduction

The determination of liquid levels in industrial vessels of process plants or tanks in automotive applications is an important measurement task in a number of today's industrial processes. Traditional level sensors are mechanical devices like floaters, hydrostatic pressure sensors, capacitive tubular sensors or ultrasound/radar based time of flight sensors. In a number of industrial processes the used fluids are mixtures or emulsions of different media. In tanks this emulsions separate due to the different densities of the components. In this case traditional sensors fail. Recently, the application of methods out of electrical capacitance tomography has been presented for noninvasive capacitive level sensors to determine stacked liquid layers [1]. Typically, noninvasive capacitive level sensors take use of the almost linear signal trend obtained by the different sensor segments when the liquid level is crossing the specific segment [2], [3]. Hence, the methods are not applicable for stacked liquid layers. However, the linear trend is also a matter of the arrangement of the electrodes. It has also been reported in [1], that for other electrode arrangements far more complex signal trends can be observed. Due to the complex signal trends, the application of more powerful model based algorithms to obtain phase boundaries between different immiscible fluids seems suitable. In this work we investigate the behavior of three different electrode arrangements for level determination of tanks using methods from electrical capacitance tomography. All schemes have in common that the number of receiver electrode is low in order to keep the installation costs low. The schemes simulated for two different tank systems in order to evaluate the sensitivity against changes in the environment. Further the application of a full tomographic approach is investigated.

II. Modeling of a Tank system

Aim of this section is to provide information about the modeling of a tank system for field numeric simulations, which is used for the further investigations. Figure 1 depicts a generic scheme of the tank system for the investigations. For clarity some components of the system are not depicted in figure 1. The tank is of cylindric form with a total hight of 300 mm and an interior diameter of about 90 mm. The tank wall. which is not depicted in figure 1 is made out PVC material with a thickness of 5 mm. The electrodes of the level sensor are put in direct contact with the sensor wall, as can be seen in figure 1. A grounded screen is placed in close distance behind the electrodes. On the ground level of the tank an electrode is placed, which is used to model the electrical behavior of a grounded drainage. We refer to electrical floating tanks as *tank 1* (in this case the ground electrode is inactive) and *tank 2* for grounded case. In the second case of a drainage is electrically connected to the ground potential (the screen) of the sensor due to the installation.
The governing partial differential equation to describe the electrical effects in the system is given by the potential equation

$$\nabla \cdot (\varepsilon_0 \varepsilon_r \nabla \Phi) = 0, \tag{1}$$

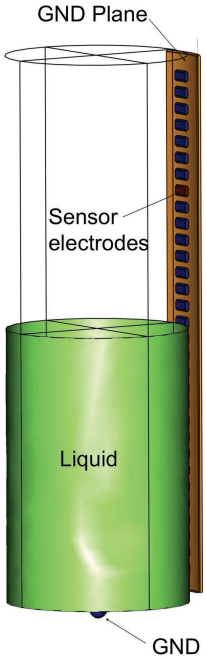

Fig. 1. Illustration of the simulation model.

where Φ is the electric scalar potential and $\varepsilon_0\varepsilon_r$ is the permittivity. On the electrodes Dirichlet type boundary conditions given by

$$\Phi_{\Gamma_{R,i}} = 0\,\mathrm{V} \qquad \forall i, \tag{2}$$

$$\Phi_{\Gamma_{Sreen}} = 0\,\mathrm{V}, \tag{3}$$

$$\Phi_{\Gamma_T} = V_0, \tag{4}$$

are applied, where Γ_T denotes the surface of the active electrode and Γ_{Screen} and $\Gamma_{R,i}$ denote the surfaces of the grounded electrodes and the screen. On the far boundary we applied a distributed capacitance formulation given by

$$-\vec{n}\vec{\boldsymbol{D}} = \varepsilon_0\varepsilon_r \frac{V_{ref} - \Phi}{d}, \tag{5}$$

where d denotes the thickness of a synthetic layer, which is terminated by a Dirichlet type boundary condition of potential V_{ref}. This boundary condition is crucial for the successful simulation of the system. In finite element schemes, the boundary of the problem is typically set away from the regions of high gradients (the sensor), to avoid large interactions between the boundary and the object (region) of interest. However, due to its large surface and the possibly high permittivity values (i.e. water), the tank acts like a large electrode. Hence, the far boundary needs an increased distance, which comes with increased computational costs. As the boundary condition (5) determines the normal component of the flux, it turned out, that by this formulation the boundary can be modeled in close distance to the tank, which saves computation time due to the decreased number of finite elements. After solving (1) for the boundary conditions, the trans-capacitances are computed by Gauss's law.

III. Different sensor topologies and behaviors

A. Sensor topologies

In this section three different electrode schemes are presented, which are under investigation. The schemes are motivated by the recent availability of capacitance measurement ICs, which typically feature the required setup of several transmitter electrodes and a low number of receiver electrodes [4]. Figure 2 depicts the three schemes. Scheme 1, which is depicted in figure 2(a), is the traditional scheme for a planar level sensor. Scheme 2 is depicted in figure 2(b). In this scheme receiver and transmitter electrodes follow each other. Figure 2(c) depicts scheme 3, in which two receiver electrodes are within the transmitter electrodes. As the electrical lines of receiver electrodes require a more expensive cabling and guarding to avoid inference from the transmitter lines, the presented schemes are in general preferable, as they are less expensive.

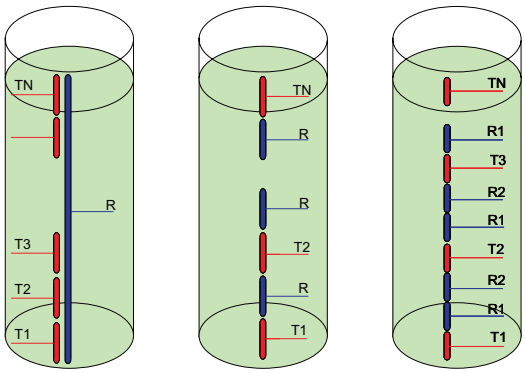

(a) Electrode scheme 1. (b) Electrode scheme 2. (c) Electrode scheme 3.

Fig. 2. Different electrode schemes possible for capacitive level determination.

B. Sensor behavior

Figure 3 depict the normalized and offset corrected trends of the simulated capacitances when the tank is filled with either a liquid of low permittivity as well as a liquid with a high permittivity for the floating and grounded case. The left sided plot in figure 3 depict the signal in the not grounded case (tank 1), whereas the right sided plots depict the case where the liquid is grounded (tank 2), which means that the liquid is electrically connected to the ground potential of the sensor. Further, the (normalized) sum of all capacitances is plotted as black line (bold for the low permittivity material and dashed for the low permittivity material) in all plots. Observing the sum signal for the not grounded case, it can be seen that scheme 1 provides an excellent linear behavior, which is basically the reason for the use of this electrode scheme in traditional level sensors. The cumulated trends of the two other schemes offer an almost linear behavior, but the trends are corrupted by an oscillating behavior, as can be observed in the figures 3(c) and 3(e). Futher, the

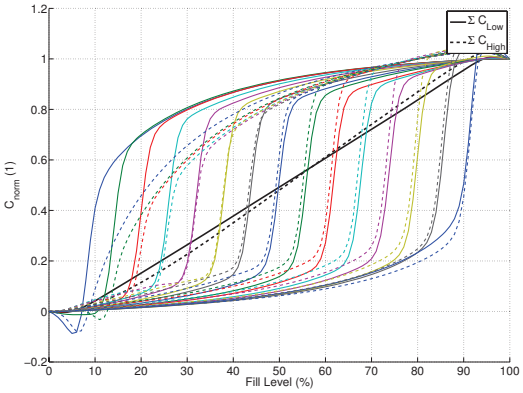

(a) Scheme 1: not grounded case.

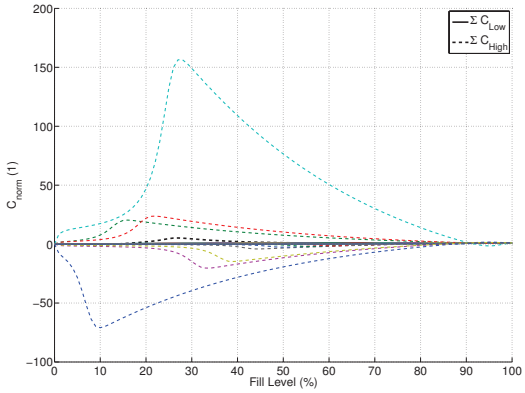

(b) Scheme 1: grounded case.

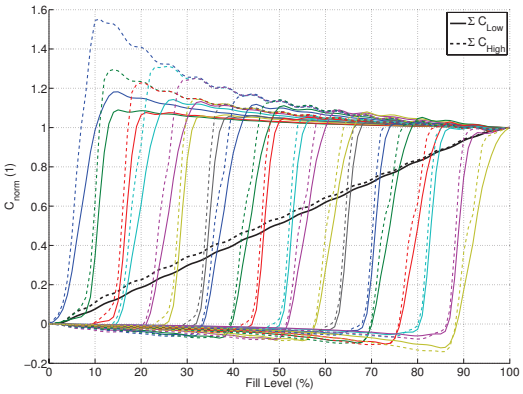

(c) Scheme 2: not grounded case.

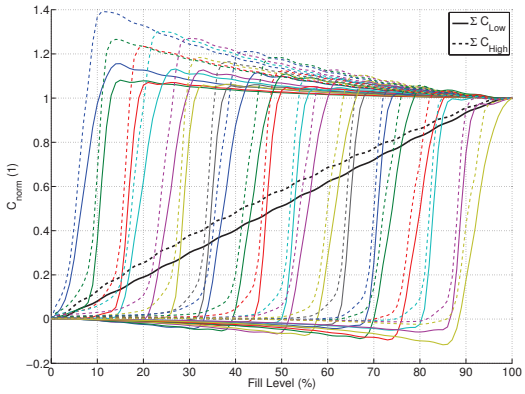

(d) Scheme 2: grounded case.

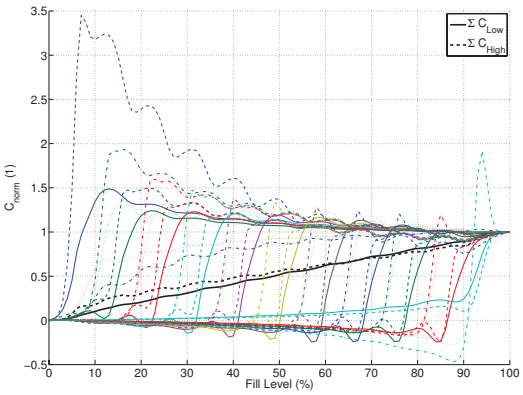

(e) Scheme 3: not grounded case.

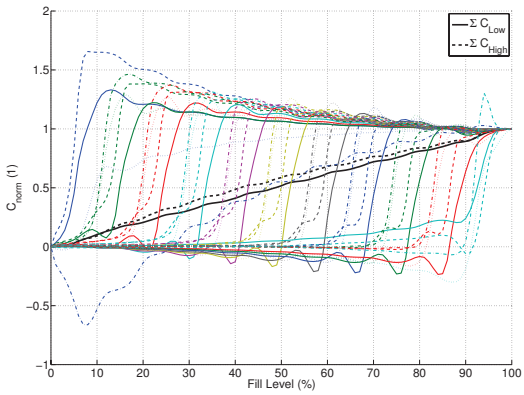

(f) Scheme 3: grounded case.

Fig. 3. Signal trends for the schemes.

schemes 2 and 3 offer a far more complex signal interaction compared to the s-like signal trends of scheme 1, which are depicted in figure 3(a). Another interesting fact can be observed in 3(b). In the grounded case scheme 1 fails for a liquid with high permittivity. This can be explained by the increased coupling behavior of the large electrode in this arrangement.

IV. Electrical Capacitance Tomography for Level Determination

After the investigations about the sensor behavior in the previous section, this section deals with the application of methods from electrical capacitance tomography for the determination of the fill level and further the

determination of stacked liquids. The interest also lies in the sensitivity towards unknown tank conditions (i.e. whether the tank grounded or not).

A typical approach to solve the nonlinear inverse problem of electrical capacitance tomography is given by a least squares fit of the form

$$\boldsymbol{h}^* = \arg\min_{\boldsymbol{h}} \left\{ ||\boldsymbol{C}(\boldsymbol{h}) - \boldsymbol{C}_{meas}||^2 \right\}, \tag{6}$$

where it is aimed to vary the fill level vector $\boldsymbol{h}$ in such a way, that the squared error between the measured capacitances $\boldsymbol{C}_{meas}$ and a model output $\boldsymbol{C}(\boldsymbol{h})$ becomes a minimum. Figure 4 depicts the normalized trends of (6) for the three schemes. In all three cases the sensor assumes a liquid with low permittivity and a not grounded tank (tank 1) and the trends depict the behavior of (6) for the correct and the opposite cases. The true fill level was in the mid level of the tank.

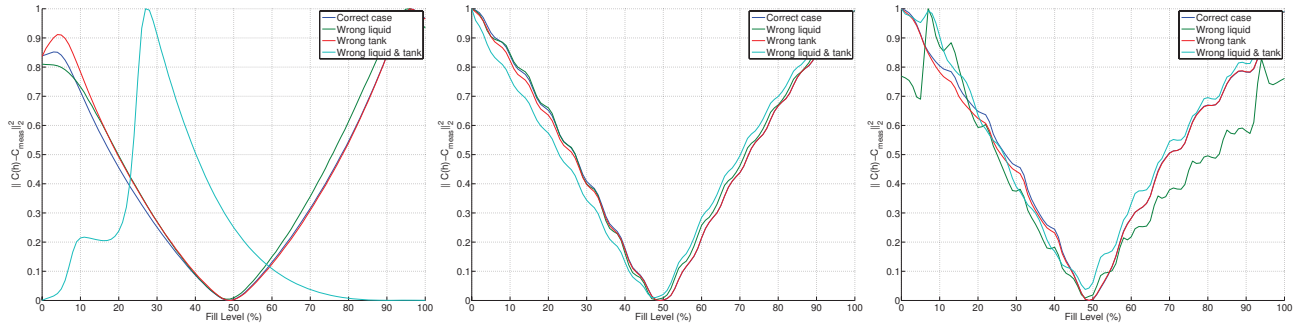

(a) Scheme 1. (b) Scheme 2. (c) Scheme 3.

Fig. 4. Error trends for the different schemes.

Expect the case of the high permittivity liquid in the grounded case for scheme 1, all trends lead to a minimum close to the true level. However, as scheme 1 fails, the application of it in the general scheme is critical in this case. The trends for scheme 2 and scheme 3 offer several minima due to the oscillating signal trends, which had been reported in the previous section. This has to be considered when finding the solution of (6).

The more interesting application lies in the determination of a stacked liquid, i.e. the determination of an oil layer on water. In this case (6) has to be extended to

$$\begin{bmatrix} h^*_{water} & h^*_{oil} \end{bmatrix} = \arg \min_{\begin{bmatrix} h_{water} & h_{oil} \end{bmatrix}} ||\boldsymbol{C}(h_{water}, h_{oil}) - \boldsymbol{C}_{meas}||_2^2. \tag{7}$$

As scheme 1 failed for liquids with high permittivity in the grounded case, the following investigations are made for scheme 2 and scheme 3. In the following the behavior of (7) is depicted in form of an error surface plot, which means that $||\boldsymbol{C}(h_{water}, h_{oil}) - \boldsymbol{C}_{meas}||_2^2$ is plotted as a function of h_{water} and h_{oil} in the region of the true values of h_{water} and h_{oil}. Figure 5 depicts the error surface of (7) for scheme 2 for the not grounded and the grounded case of the tank, under the assumption that the tank is not grounded. The red dots in both plots of figure 5 mark the true values of the hight of the water and the oil layer on it. One can observe a flat behavior of the error surface. However, in the case of the not grounded tank, the minimum can be found. In the grounded case algorithm (7) provides a biased result. Figure 6 depicts the same for scheme 3. Again, the result is biased in the case of the wrong tank. However, the error curve in the correct case offers a more distinct minimum. The flat behavior of the error surface given by (7) is still a negative behavior in the tomographic approach when applied to the presented electrode schemes. Hence, the properties of a full tomographic approach are of interest. Full tomographic means, that all inter-electrode capacitances are measured. For this, the electrode arrangement of the schemes 2 and 3 is used. Figure 7 depicts the simulated error curves for the full tomographic case. The simulations were carried out on a 2D model. Figure 7(a) again depicts the not grounded case, figure 7(b) depicts the case of a grounded tank under the opposite assumption. Again, the error curves offer a flat behavior in the target region. However, in the grounded case

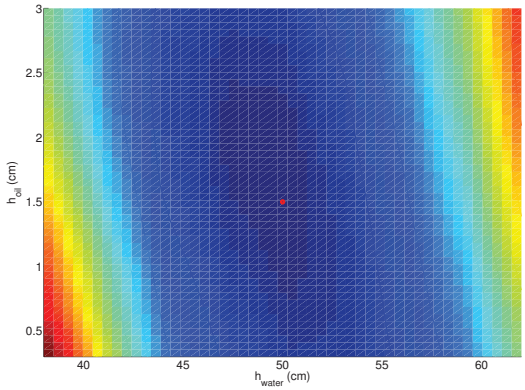

(a) Tank not grounded.

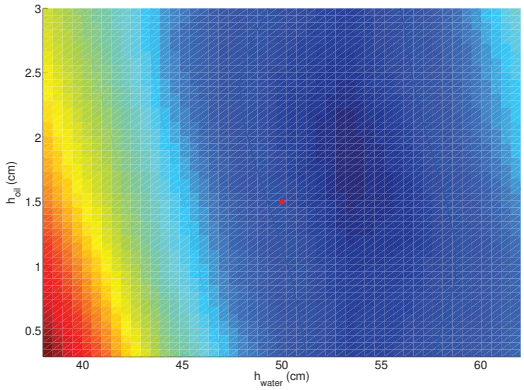

(b) Tank grounded.

Fig. 5. Error surface for the determination of a liquid stack for scheme 2.

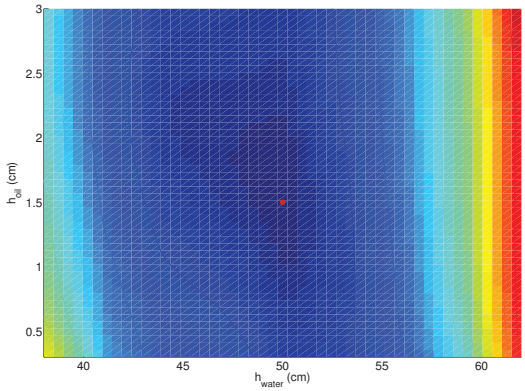

(a) Tank not grounded.

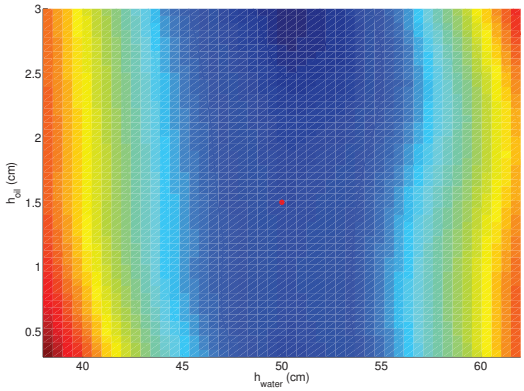

(b) Tank grounded.

Fig. 6. Error surface for the determination of a liquid stack for scheme 3.

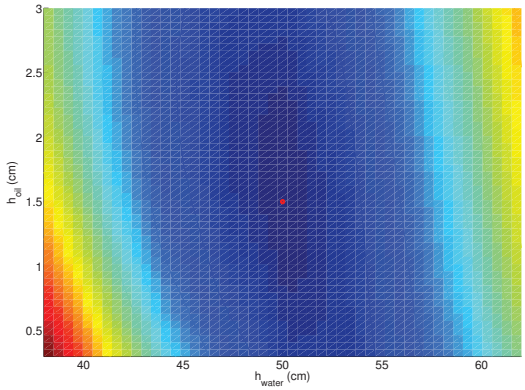

(a) Tank not grounded.

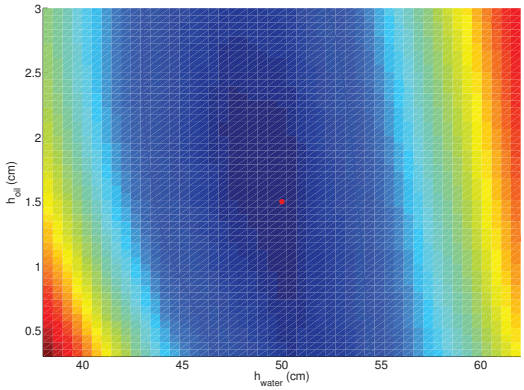

(b) Tank grounded.

Fig. 7. Error surface for the determination of a liquid stack in the full tomographic case (2D simulation).

also a minimum close to the true values appears. Hence, the electrode scheme in combination with the full tomographic reconstruction approach appears more robust with respect to changed environmental conditions.

V. Conclusion

In this work the application of electrical capacitance tomography low liquid level measurements has been presented. The results propose the applicability of the methods from electrical capacitance tomography, although the application of capacitive sensor has always to be in concern with the sensor environment. Thus, further research will focus on the design of robust electrode layouts and further improvements of the algorithms to be able to determine and react on changed environmental conditions.

References

[1] M. Neumayer and H. Zangl, Modeling of a Tank System for Liquid Level Measurement by Means of Electrical Tomography, 6th World Congress on Industrial Process Tomography (WCIPT6), Beijing, China, 6-9 September 2010.

[2] Toth F.N.; Meijer, G.C.M.; van der Lee, M., (1997), A planar capacitive precision gauge for liquid-level and leakage detection, IEEE Transactions on Instrumentation and Measurement, vol. 46, no.2, pp. 644-646.

[3] Mohr, T.; Ehrenberg, U.; Uhlmann, H., (2001), A new method for a self-calibrating capacitive sensor, Proceedings of the 18th IEEE Instrumentation and Measurement Technology Conference, vol.1, pp. 454-459.

[4] Analog Devices, (2007), AD7143 - Programmable Controller for Capacitance Touch Sensors.